Full Paper

Wiley Online Library

ELECTROANALYSIS

DOI: 10.1002/elan.201800034

Non-Covalent Functionalization of Multi-Wall Carbon Nanotubes with Polyarginine: Characterization and Analytical Applications for Uric Acid Quantification

Alejandro Gutiérrez,[a, b] Fabiana Gutierrez,[a] Marcos Eguílaz,[a] Concepción Parrado,[c] and Gustavo A. Rivas*[a]

Abstract: We report for the first time the non-covalent functionalization of multiwall carbon nanotubes (MWCNTs) with polyarginine (Polyarg), the modification of glassy carbon electrodes (GCE) with the resulting Polyarg-MWCNTs dispersion and the analytical application of Polyarg-MWCNTs-modified GCE for the quantification of uric acid. The optimum MWCNT-Polyarg dispersion was obtained by sonicating for 5.0 min the mixture of 0.75 mg mL^{-1} MWCNTs and 0.50 mg mL^{-1} Polyarg. The dispersion was characterized by scanning electron microscopy, electrophoretic mobility, electrochemical impedance spectroscopy, cyclic voltammetry and amperometry. The presence of MWCNT-Polyarg at GCE surface produced a drastic decrease in the overvoltages for the oxidation of hydrogen peroxide (300 mV) ascorbic acid (281 mV) and uric acid (70 mV) and for the reduction of hydrogen peroxide (200 mV), as well as an important decrease in the charge transfer resistances for hydrogen peroxide, hydroquinone/quinone and ferricyanide/ferrocyanide markers. The strong adsorption of uric acid at GCE/MWCNT-Polyarg made possible the highly sensitive detection of this biomarker at nanomolar levels even in the presence of 1.0×10^{-4} M ascorbic acid by Adsorptive Stripping with medium exchange and linear scan voltammetry transduction. The quantification of uric acid in untreated human urine was very successful, demonstrating an excellent correlation (98%) with the reference method used in clinical laboratories (Uricostat, Wiener Lab).

Keywords: Carbon nanotubes functionalization · Polyarginine · Electrochemical sensor · Ascorbic acid · Uric acid sensor

1 Introduction

The discovering of carbon nanomaterials has demonstrated to be a key point for the development of the nano (bio)technology. In particular, carbon nanotubes (CNTs) have attracted enormous attention for the design of new sensing technologies due to their unique physical, electronic, and chemical properties [1–5]. Owing to their outstanding beneficial characteristics and their ability to promote electron transfer reactions, CNTs have been successfully used for the development of a large number of electrochemical (bio)sensors, as it has been extensively reviewed in the literature [6–8]. However, the important interactions between CNTs make difficult their direct application for the development of electrochemical sensors [9,10]. Therefore, a functionalization step, either covalent or non-covalent, is highly required, and the performance of the resulting sensors is extremely dependent on the efficiency of this functionalization. In this regard, the use of (bio)polymers as CNTs-functionalization agents have demonstrated to be extremely useful [11,12]. We have reported the use of polyethylenimine [13,14], polylysine [15,16], polyhistidine [17,18], glucose oxidase [19], calf-thymus double stranded DNA [20,21] and cytochrome c [22] for the highly successful non-covalent functionalization of multi-wall carbon nanotubes (MWCNTs). Polytyrosine covalently attached to single-wall carbon nanotubes (SWCNTs) have also demonstrated to be highly effective for the preparation of electrochemical sensors [23].

In this work we are reporting the non-covalent functionalization of MWCNTs based on the use of polyarginine (Polyarg) as dispersing agent and the development of an uric acid (UA) electrochemical sensor through the modification of glassy carbon electrodes (GCE) with the resulting MWCNTs-Polyarg dispersion.

UA is the main final product of purine metabolism in the human body and is an important biomarker. In fact, abnormal levels in blood are usually connected with

[a] A. Gutiérrez, F. Gutierrez, M. Eguílaz, G. A. Rivas
INFIQC, Departamento de Fisicoquímica, Facultad de Ciencias Químicas, Universidad Nacional de Córdoba, Ciudad Universitaria, 5000 Córdoba, Argentina
Phone: +54-351-5353866; Fax: +54-351-4334188
E-mail: grivas@fcq.unc.edu.ar

[b] A. Gutiérrez
División de Estudios de Posgrado e Investigación, Instituto Tecnológico de Cd. Madero, J. Rosas y J. Urueta S/N Col. Los Mangos, Cd. Madero, Tamaulipas, C.P. 89440, México

[c] C. Parrado
Departamento de Química Analítica, Facultad de Ciencias Químicas, Universidad Complutense de Madrid, Madrid, Spain

Supporting information for this article is available on the WWW under https://doi.org/10.1002/elan.201800034

diseases like gout, hyperuricaemia, Lesch–Nyhan syndrome [24] and cardiovascular disorders [25]. Considering the significance of these pathologies, the development of methodologies that allow the sensitive and selective quantification of UA is highly required. Electrochemical sensors have demonstrated to be very useful for sensing different bioanalytes [26,27]; however, the major problem in the electrochemical detection of UA is the coexistence of interfering compounds, mainly ascorbic acid (AA), since it oxidizes at potentials close to UA oxidation, making very difficult their selective quantification. Thus, one important challenge in the electrochemical sensing of UA is the development of new strategies that make possible the detection of UA in the presence of AA or at least the discrimination between the oxidation processes of both analytes.

This work presents a first section where discussing the influence of the sonication time and the amount of Polyarg and MWCNTs on the efficiency of the dispersions using common redox markers like hydrogen peroxide and AA, and a second section where presenting the analytical application of glassy carbon electrodes (GCEs) modified with the resulting dispersion (GCE/MWCNT-Polyarg) for the sensitive and selective quantification of UA in the presence of AA.

2 Experimental

2.1 Reagents

Poly-L-arginine hydrochloride (Polyarg) (mol wt > 70,000) and hydroquinone (H_2Q) were obtained from Sigma. Hydrogen peroxide (H_2O_2, 30 % v/v aqueous solution) and ascorbic acid (AA) were purchased from Baker. Potassium ferrocyanide, potassium ferricyanide and uric acid (UA) were supplied by Merck. Multiwalled carbon nanotubes (MWCNTs) of 15–45 nm diameter and 1–5 microns length were obtained from NanoLab (USA). Other chemicals were analytical reagent grade and used without further purification. Ultrapure water ($\rho =$ 18 MΩ cm) from a Millipore-MilliQ system was used to prepare all the solutions. The stock solutions of AA and UA were prepared in a 0.050 M phosphate buffer pH 7.40 before starting each set of experiments, stored in ice bath, and covered with alumina foil until using. Polyarg solutions were prepared in water.

2.2 Apparatus

Sonication treatments were carried out with an ultrasonic processor VCX 130 W (Sonics and Materials, Inc.) of 20 kHz frequency with a titanum microtip (3 mm diameter). A Digicen 21 ultracentrifuge (Orto Alresa) with a RT 151 rotor was used to centrifuge the samples after sonication.

Amperometric and voltammetric measurements were performed with EPSILON (BAS) and TEQ_02 potentiostats. The electrodes were inserted into the cell (BAS, Model MF-1084) through holes in its Teflon cover. A platinum wire and Ag/AgCl, 3 M NaCl (BAS, Model RE-5B) were used as counter and reference electrodes, respectively. All potentials are referred to the latter. A magnetic stirrer provided the convective transport during the amperometric measurements.

EIS experiments were performed by applying a sinusoidal potential perturbation of 10 mV of amplitude in the frequency range of 10^5–10^{-1} Hz using different redox markers: 2.0×10^{-3} M Q/H_2Q, 2.50×10^{-2} M H_2O_2 and 2.0×10^{-3} M $[Fe(CN)_6]^{3-/4-}$. The working potentials were 0.700 V for hydrogen peroxide, and the formal potential for Q/H_2Q (~0.05 V) and $Fe(CN)_6]^{3-/4-}$ (~0.20 V) solutions. The impedance spectra were analyzed and fitted by using the Z-view program.

Scanning electron microscopy (SEM) images were obtained with a Field Emission Gun Scanning Electron Microscope (FE-SEM, Zeiss, ΣIGMA model).

The zeta potential (z) was determined by electrophoretic light scattering (ELS) measurements, using a Delsa Nano C instrument (Beckman Coulter).

2.3 Preparation of Glassy Carbon Modified Electrodes

2.3.1 Preparation of MWCNTs-Polyarg Dispersion

0.75 mg of MWCNTs were mixed with 1.00 mL of 0.50 mg mL^{-1} Polyarg solution followed by sonication for 5.0 min with ultrasonic probe. Finally, the dispersion was centrifuged for 15 min at 9000 rpm and the supernatant was collected for further work.

2.3.2 Modification of Glassy Carbon Electrodes (GCE) with MWCNT- Polyarg (GCE/MWCNT-Polyarg) and Polyarg (GCE/Polyarg)

Before modification, the GCEs were polished with alumina slurries of 1.0, 0.30, and 0.05 μm for 1.0 min each. After polishing, the electrodes were rinsed with water and cycled 10 times in 0.050 M phosphate buffer solution between −0.200 V and 0.800 V at 0.100 V s^{-1}. Finally, an aliquot of 10 μL of MWCNT-Polyarg (supernatant) or 1.00 mg mL^{-1} Polyarg were dropped on the top of the polished GCEs, allowing the solvent to evaporate for 60 min at room temperature.

2.4 Quantification of UA

The quantification of UA was performed by Adsorptive stripping analysis with medium exchange and Linear Scan Voltammetry (LSV) transduction according to the following procedure:

(I) Preconcentration: performed at open circuit potential by immersion of GCE/MWCNT-Polyarg in the UA solution (prepared in a 0.050 M phosphate buffer solution pH 7.40) for 5.0 min under stirring conditions.

(II) Washing: the electrodes containing the accumulated material were washed with a 0.050 M phosphate

buffer solution pH 7.40 for 10 s and then transferred to a fresh phosphate buffer solution.

(III) Transduction: The anodic stripping was performed in a 0.050 M phosphate buffer solution pH 7.40 by scanning the potential between −0.300 V and 0.600 V at 0.050 $V s^{-1}$ using LSV. The analytical signals were obtained from the oxidation peak currents of UA after subtracting the background currents. All measurements were performed at room temperature.

2.5 Validation of the Sensor

The sensor was validated with the Uricostat enzymatic kit from Wiener Lab (Argentina), a reference method for the quantification of UA in clinical laboratories [28]. This method is based on the use of uricase to convert UA into allatoin in the presence of oxygen which, in turn, is reduced to hydrogen peroxide (reaction 1). In the second step, the enzymatically generated hydrogen peroxide in the presence of peroxidase, 4-aminophenzone and dichloro-hydroxy bencensulfonic acid generates quinoimine (reaction 2), compound that absorbs at 505 nm. The absorbance of this compound is used as analytical signal. Urine samples were collected for 24 h and used untreated for the quantification of UA.

$$UA + 2H_2O + O_2 \rightarrow \text{allatoin} + H_2O_2 + CO_2 \quad \text{[reaction 1]}$$

$$H_2O_2 + \text{4-AF} + \text{DCHBS} \rightarrow \text{quinonimine} \quad \text{[reaction 2]}$$

Where 4-AF: 4-aminophenazone, DCHBS: dichlorohydroxybencen sulfonic acid.

3 Results and Discussion

3.1 Characterization of MWCNT-Polyarg Dispersions

Figure S1 displays a SEM image of a glassy carbon disk modified with MWCNTs non-covalently functionalized with Polyarg (0.75 mg mL^{-1} MWCNTs/0.50 mg mL^{-1} Polyarg sonicated for 5.0 min). The image reveals a complete coverage of the glassy carbon surface although, as in other MWCNTs-polymer modified GCEs [11], there are areas with different density of MWCNTs.

The dispersions were also characterized by different electrochemical techniques. The electronic properties of GCE/MWCNT-Polyarg were comparatively evaluated with those of GCE and GCE/Polyarg by EIS using quinone/hydroquinone (Q/H_2Q), H_2O_2, and $[Fe(CN)_6]^{-3/-4}$ as redox markers. Figure 1 displays Nyquist plots obtained for the different redox markers and electrodes. The symbols correspond to the experimental points and the solid lines to the fitting with the corresponding equivalent circuits, which are shown in Figure S2. Figure 1A depicts the Nyquist plots obtained at 0.050 V for GCE (a), GCE/Polyarg (b) and GCE/CNT-Polyarg (c) using 2.0×10^{-3} M Q/H_2Q as marker, and a Randles (a and c) or ($R_s(R_{ct}C_{dl})$) (b) circuits. The inset shows a bars plot for the charge

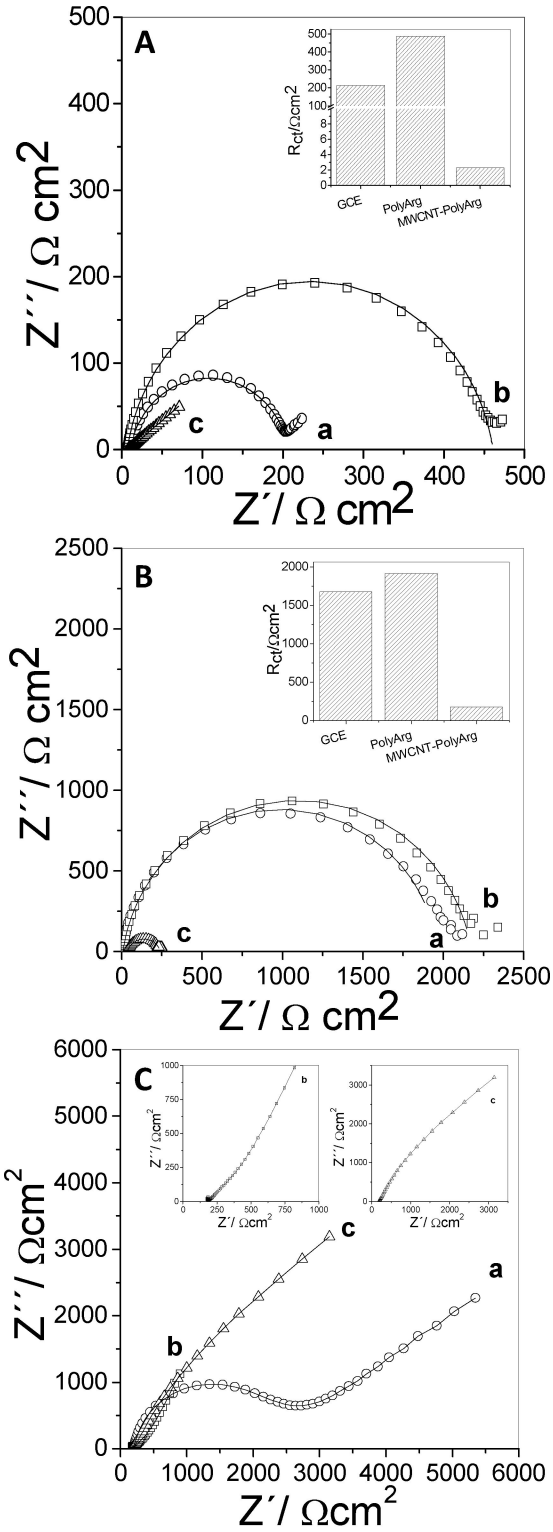

Fig. 1. Nyquist plots for 2.0×10^{-3} M Q/H_2Q (A), 2.5×10^{-2} M H_2O_2 (B) and 2.0×10^{-3} M $[Fe(CN)6]^{3-/4-}$ (C) obtained at GCE (a), GCE/Polyarg (b) and GCE/MWCNT-Polyarg (c). Working potential: A) 0.050 V, B) 0.700 V and C) 0.200 V. Frequency range: 10 KHz to 10 mHz; Potential perturbation: 10 mV; Supporting electrolyte: 0.100 M phosphate buffer solution pH 7.40. Insets Figures 1A and B: bar plots for the Rct obtained at the different electrodes; Inset Figure 1C zoom of the spectra obtained at higher frequencies.

transfer resistance (R_{ct}) obtained at the different electrodes. Since Q/H_2Q needs to be adsorbed at sp^2 carbon to allow the charge transfer at the electrode, the electrochemical response of this redox couple is very sensitive to the surface blockage [29].Taking into account that the semicircle portion at high frequencies corresponds to the charge transfer limited processes, is evident that R_{ct} increases when GCE is modified with Polyarg due to the blockage of the surface (214 and 487 $\Omega\,cm^2$ for GCE and GCE/Polyarg, respectively). On the contrary, the modification of GCE with MWCNTPolyarg produces a drastic decrease of R_{ct} (2.3 $\Omega\,cm^2$) suggesting that, even when the polymer that supports the CNTs has a passivating effect, the electroactivity of CNTs makes possible a huge increment in the charge transfer rate of the redox marker.

For better comprehension of the electrochemical behavior of GCE modified with MWCNT-Polyarg, the system was also evaluated using H_2O_2 as redox marker. Figure 1B displays Nyquist plots obtained in a 2.5×10^{-2} M hydrogen peroxide solution at 0.700 V using GCE (a), GCE/Polyarg (b) and GCE/MWCNT-Polyarg (c). The inset depicts a bars plot for the R_{ct} obtained at the different surfaces. In this case, the experimental data were satisfactorily fitted with the simple equivalent circuit ($R_s(R_{ct}C_{dl})$). Since the charge transfer of hydrogen peroxide is not as sensitive as H_2Q/Q to the state of the electrode surface, the R_{ct} at GCE/Polyarg slightly increases compared to GCE; however, as in the previous case, R_{ct} largely decreases when GCE is modified with MWCNT-Polyarg due to the efficient catalytic activity of the CNTs towards hydrogen peroxide oxidation (1678, 1913 and 176 $\Omega\,cm^2$ for GCE, GCE/Polyarg and GCE/MWCNT-Polyarg, respectively).

EIS experiments using the highly-charged redox couple $[Fe(CN)_6]^{3-/4-}$as redox marker were also performed at 0.200 V to study the effect of the charge of MWCNT-Polyarg on the electron transfer of the anion. Nyquist plots for GCE showed a typical resistive component at high frequencies and a diffusional one at lower frequencies, using ($R_s(R_{ct}C_{dl})$) circuit (a). In the presence of Polyarg, R_{ct} drastically decreases due to the electrostatic attraction between the negatively charged marker and the positively charged dispersion, demonstrating that the polymer that supports the MWCNTs facilitates the apparent charge transfer of the probe. It is important to mention that ζ potential for MWCNT-Polyarg in a 0.050 M phosphate buffer solution was (0.0530 ± 0.006) V, indicating that the dispersion presents a positive charge under the working conditions. In this case, the experimental data were satisfactorily fitted with the modified Randles circuit indicated in Figure S2,C which also includes a pseudocapacitance. This capacitive behavior observed at lower frequencies, is associated with the adsorption of the redox probe. No significant differences in R_{ct} were observed at GCE/MWCNT-Polyarg compared to GCE/Polyarg, although the presence of MWCNT-Polyarg produces important changes in the diffusional portion of Nyquist plots due to diffusional problems associated with the film thickness of MWCNT-Polyarg.

Figure 2 shows cyclic voltammograms for 5.0×10^{-2} M H_2O_2 (A), 1.0×10^{-3} M AA (B) and 1.0×10^{-4} M UA (C) obtained at GCE (dotted line) and GCE/MWCNTs-Polyarg (solid line). The voltammetric response for hydrogen peroxide at MWCNTs-Polyarg modified GCE shows a huge enhancement in the reduction/oxidation currents and a very important decrease in the oxidation (300 mV) and reduction (200 mV) overvoltages compared to bare

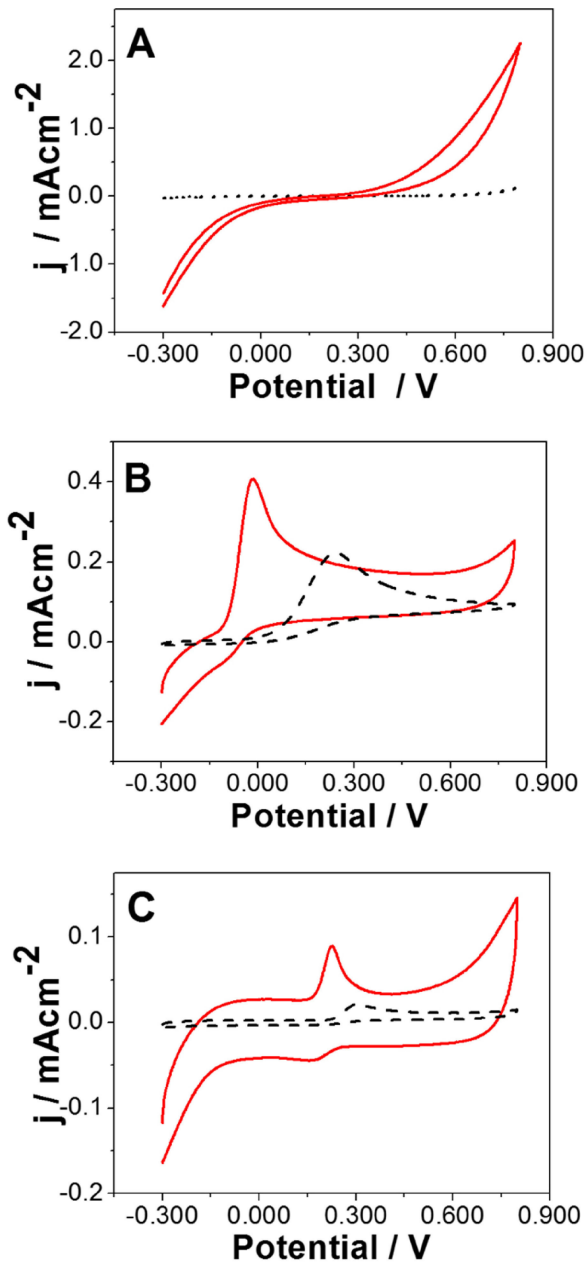

Fig. 2. Cyclic voltammograms for 0.050 M hydrogen peroxide (A), 1.0×10^{-3} M AA (B) and 1.0×10^{-4} M UA (C) at GCE (dotted line) and GCE/MWCNT-Polyarg (solid line). Scan rate: 0.050 $V\,s^{-1}$. Supporting electrolyte: 0.050 M phosphate buffer solution pH 7.40.

GCE, in consonance with the EIS results previously described (Figure 1B). The potentiodynamic profiles for 1.0×10^{-3} M AA solution at GCE/MWCNT-Polyarg show a decrease of 281 mV in the oxidation overvoltage compared to GCE, as a result of the catalytic activity of MWCNTs and the facilitated interaction of the negatively charged ascorbate with the positively charged MWCNT-Polyarg dispersion (Figure 2B). As Figure 2C displays, these effects are also evident for the electrooxidation of UA, compound that is negatively charged under our working conditions. In fact, at GCE/MWCNT-Polyarg the oxidation overvoltage for UA decreases 70 mV and the peak current enhances in a factor of 5.

3.2 Optimization of MWCNT-Polyarg Dispersions

As it was previously reported [11], one of the crucial aspects when developing CNTs-based electrochemical (bio)sensors is to find a strategy that allows an efficient and stable functionalization of the nanostructures, their successful dispersion in aqueous media, and a deposition at electrode surfaces in a homogeneous and robust way.

We evaluated the influence of the amount of MWCNT, the concentration of Polyarg and the sonication time on the efficiency of the dispersion by cyclic voltammetry and amperometry using hydrogen peroxide as redox marker.

Figure 3A shows the effect of the concentration of Polyarg on the sensitivity to hydrogen peroxide obtained from amperometric experiments at 0.700 V using GCE modified with dispersions of MWCNTs (0.75 mg mL^{-1}) in Polyarg solutions of different concentration (from 0.25 to 2.00 mg mL^{-1}). The sensitivity obtained at bare GCE is also included for comparison. The sensitivity largely increases when GCE is modified with MWCNT-Polyarg dispersions prepared either with 0.25, 0.50 or 1.00 mg mL^{-1} Polyarg, demonstrating the efficiency of Polyarg as dispersing agent. Dispersions prepared with 2.0 mg mL^{-1} Polyarg produced a decrease in the sensitivity due to the passivating effect of the polymer at high concentrations. Therefore, 0.50 mg mL^{-1} Polyarg was selected as the optimum amount of Polyarg to efficiently disperse 0.75 mg mL^{-1} MWCNT in water after 5.0 min sonication. It is important to mention that the selected solvent was water since it allowed the best compromise between the quality of the dispersion, the robustness of the deposited layer at the GCE, and the reproducibility of the amperometric response of the resulting sensor.

The effect of the amount of MWCNTs was evaluated using 0.50 mg mL^{-1} Polyarg (Figure 3B) and hydrogen peroxide as redox marker. As in the previous case, the sensitivity obtained at GCE was also included for comparison. A large enhancement in sensitivity is observed as the amount of CNTs increases from 0.25 to 0.75 mg mL^{-1} as a consequence of the electroactivity of the nanostructures. Higher amounts of MWCNTs in the dispersion produced a decrease in the sensitivity due to a less efficient dispersion (for this concentration of Polyarg). Therefore, 0.75 mg mL^{-1} MWCNTs was selected as the optimum amount of carbon nanostructures. Similar experiments performed with AA also confirmed the advantages of the dispersion on the electro-oxidation of AA. Figure S3 depicts the variation of the peak potential and

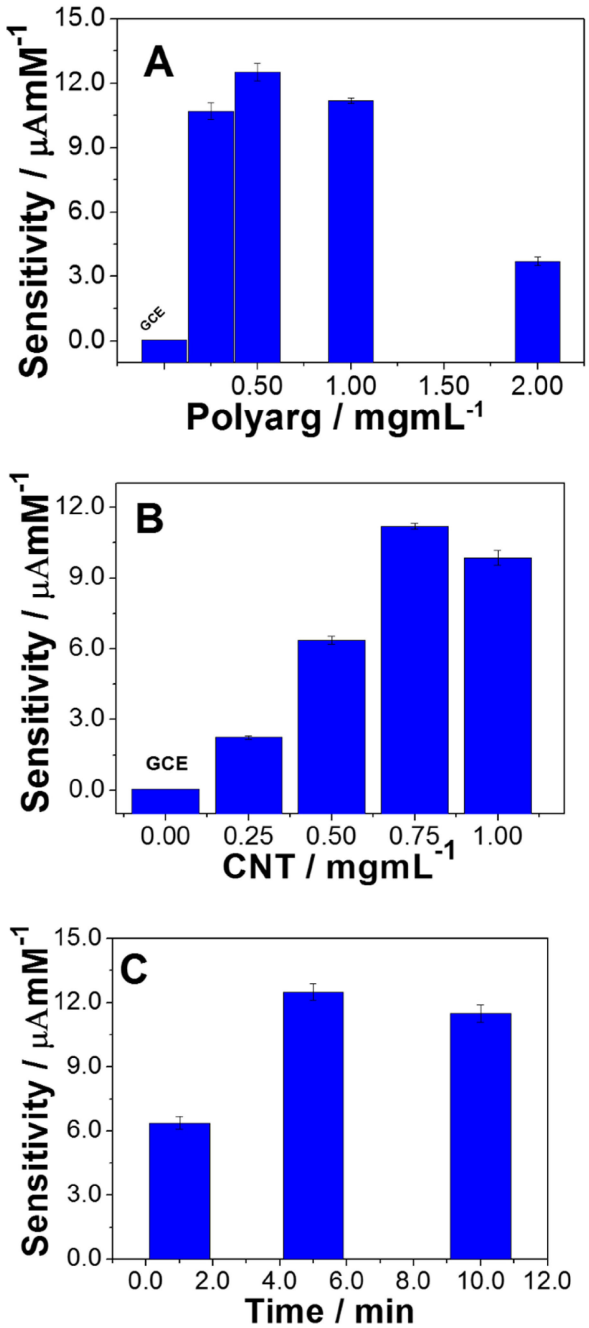

Fig. 3. Variation of the sensitivity towards hydrogen peroxide obtained from amperometric experiments performed at 0.700 V using (A) GCEs modified with MWCNTs-Polyarg dispersions prepared by sonicating for 5.0 min 0.75 mg mL^{-1} MWCNTs and different concentrations of Polyarg; (B) GCEs modified with MWCNTs-Polyarg dispersions prepared by sonicating 0.50 mg mL^{-1} Polyarg and different amounts of MWCNTs; C) GCEs modified with MWCNTs-Polyarg dispersions prepared by sonicating for different times 0.50 mg mL^{-1} Polyarg and 0.75 mg mL^{-1} MWCNTs. Other conditions as in Figure 2.

peak currents for AA oxidation obtained at GCEs modified with different amounts of MWCNTs and 0.50 mg mL^{-1} Polyarg. The presence of CNTs drastically decreases the oxidation peak potential due to their catalytic activity towards the oxidation of AA, reaching a plateau for amounts higher than 0.50 mg mL^{-1}. The peak currents increases with the amount of MWCNTs being 0.75 mg mL^{-1} the one that allows the best compromise between robustness of the dispersion and reproducibility of the signal.

It is widely known that the sonication time is an important factor when preparing CNTs-polymers dispersions since the total energy delivered by an ultrasonic probe, which depends on the applied power and the ultrasonication time, produces changes in the cavitation events chain that facilitate the separation of the nanostructures. Figure 3C shows the effect of the sonication time (between 1.0 and 10 min) on the sensitivity obtained from amperometric experiments performed at 0.700 V at GCE/MWCNT-Polyarg using hydrogen peroxide as redox marker. The sensitivity increases in a factor of 2 when the sonication time rises from 1.0 to 5.0 min, to almost level off thereafter.

In summary, the results presented here demonstrate that Polyarg is an excellent dispersing agent for MWCNT and that the best dispersion is obtained by sonicating for 5.0 min a mixture of 0.75 mg mL^{-1} of MWCNT with 0.50 mg mL^{-1} Polyarg (prepared in water).

The stability of MWCNT-Polyarg dispersion is a very important aspect for further applications in the development of sensors. Figure S4 shows the effect of the stability of MWCNTs-Polyarg stored at room temperature by evaluating the sensitivity towards the redox marker used to optimize the dispersion, hydrogen peroxide, obtained at 0.700 V at different GCEs modified with the same MWCNT-Polyarg dispersion in different days. No significant changes were observed even after 50 days storage, period at which the sensitivity remains in a 98% of the original one. The GCE/MWCNT-Polyarg also presents a very good short-term stability, with R.S.D. of 2.0% for 5 successive amperometric experiments at 0.700 V using the same electrode surface and hydrogen peroxide as marker.

3.3 Analytical Applications of GCE/MWCNT-Polyarg for the Quantification of UA

We explored the usefulness of GCE/MWCNT-Polyarg as electrochemical sensor for the quantification of UA. Figure 4 depicts potentiodynamic profiles obtained at bare GCE (a and c) and at GCE/MWCNT-Polyarg (b and d) under different conditions. While no signal is observed at bare GCE for 8.0×10^{-7} M UA without accumulation (a), at GCE/MWCNT-Polyarg (b) the oxidation current peak is (0.34 ± 0.01) μA even for such small UA concentration. After accumulation for 5.0 min in a 8.0×10^{-7} M UA solution and medium exchange to 0.050 M phosphate buffer solution pH 7.40 (c and d) the oxidation peak current at GCE/MWCNT-Polyarg increases in a factor of

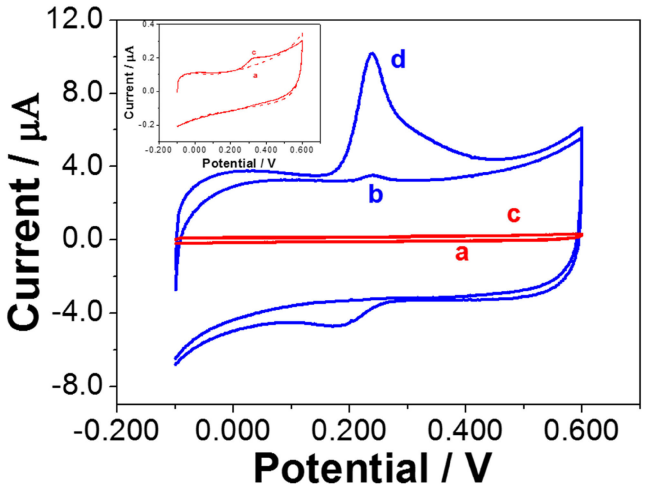

Fig. 4. Cyclic voltammograms obtained at GCE (a,c) and GCE/MWCNTs-Polyarg (b,d) under different conditions: a and b: 8.0×10^{-7} M UA without accumulation; c and d: after 5.0 minutes accumulation in a 8.0×10^{-7} M UA solution and medium exchange to 0.050 M phosphate buffer solution pH 7.40. Other conditions as in Figure 2.

100 compared to GCE after accumulation of UA using similar conditions and twenty-times compared to GCE/MWCNT-Polyarg without accumulation. This significant increment in the oxidation currents for UA clearly demonstrate the efficiency of the pre-concentration step due to the strong adsorption of UA at GCE/MWCNT-Polyarg favored by the presence of MWCNTs and the positive charge of the dispersion. The pre-concentration time that allowed the best compromise between sensitivity and reproducibility for 2.0×10^{-6} M UA was 5.0 min (not shown).

Figure 5A displays the calibration plots for UA obtained in the absence (blue squares) and in the presence (green squares) of 1.0×10^{-4} M AA, the most common interferent in the electrochemical quantification of UA. The inset shows the linear scan voltammograms obtained in a 0.050 M phosphate buffer solution pH 7.40 after 5.0 min accumulation in solutions of UA of different concentrations from 2.0×10^{-7} to 2.0×10^{-6} M at GCE/MWCNT-Polyarg. Well-defined peaks are observed in all cases. The sensitivity obtained in the absence of AA is (74.6 ± 0.4) μA M^{-1} cm^{-2} ($r=0.9998$), the linear range goes from 2.0×10^{-7} to 2.0×10^{-6} M, and the detection limit is 15 nM (taken as 3 × standard deviation of the blank signal/sensitivity). In the presence of 1.0×10^{-4} M AA the sensitivity is (79.1 ± 0.3) μA M^{-1} cm^{-2}, ($r^2=0.997$), the linear range goes from 2.0×10^{-7} to 2.0×10^{-6} M, and the detection limit is 15 nM. Therefore, the proposed sensor allows the successful quantification of UA even in the presence of a large excess of AA. Table 1 compares the analytical parameters for UA obtained using GCE/MWCNT-Polyarg and different electrochemical sensors. The results demonstrate that our sensor is highly com-

Table 1. Comparison of the analytical parameters of the proposed sensor with those for UA reported sensors.

Platform	Sample	Sensitivity ($\mu A\,\mu M^{-1}$)	Linear Range (μM)	Detection Limit (μM)	Ref.
GCE/HNP-PtTi[b]	Mixture AA, UA, DA	46.26 $\mu A\,mM^{-1}\,cm^{-2}$	100–1000	5.3	30
GCE/MWCNT/CTAB-GO[b]	AA, UA, DA, NO_3^-	0.2372	3.0–60	1.0	31
GCE/C_{60}/Pt NSs[b]	AA, UA, DA	0.0141	9.5–1187	0.63	32
GCE/MGF/MWCNT[b]	AA, UA, DA, Trp	0.2764	5–100	0.93	33
GCE/RGO/Au[b]	AA, UA, DA	0.5	8.8–53	1.8	34
GCE/RGO[b]	Urine, serum	0.0153	2–600	1.0	35
GCE/CdTe/QDs-Gr[a,b]	serum	0.1228	3–600	1.0	36
GCE/PLL/ERGO[b]	urine	0.79	20–200	0.15	37
GCE/Zeo-Y/AgNP[b]	urine	4.1	0.05–0.7	0.025	38
GCE/rGo/PAM[a]	urine	0.09433	1.0–500	0.5	39
GCE/Nafion/MWCNT/CD/HPU[f]		2.11 $\mu A\,mM^{-1}$	100–700		40
Au-IDA/Gr-FMN	Mix AA + AU	0.065	60–578	18	41
Au-IDA/Pt-Gr-FMN[a]	Mix AA + AU	0.10	60–345	18	41
GCE/CoPc/MWCNT[a]	urine	0.02	125–4000	260	42
GCE/MoS_2[a,b]	AA + DA + UA	7.1	1–60	0.06	43
GCE/Co-CeO_2[d]	HXA + UA + XA	0.0083	1–2200	0.36	44
GCE-GNs-Q-AgNPs[b]	Human urine	0.085	26.7–63.2	–	45
GCE/Mn-SnO_2[d]	Urine	0.010	1–860	0.36	46
GF@$NiCo_2O_4$[b]	Urine, serum	0.072	10–60	0.2	47
GCE/P(GBHA)[b]	Urine	0.058	1.0–100	0.09	48
GCE/C/Ni[a,b]	Human urine samples and fetal bovine serum	0.445 or 11.87 $\mu A\,\mu M^{-1}\,cm^{-2}$	5–180	0.1	49
GCE/MWCNT-Polyarg[c]	Mix AA + UA Urine	9.5	0.2–2.0	0.015	This work

Analytes (UA: uric acid, AA: ascorbic acid, DA: dopamine, Trp: Tryptophan, HXA: hypoxanthine.

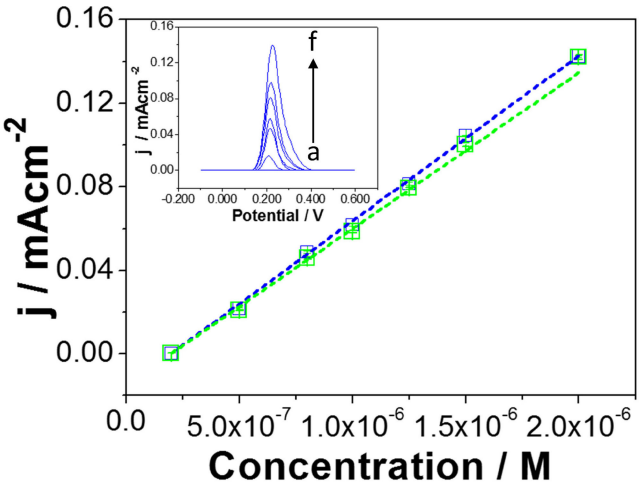

Fig. 5. Calibration plots obtained for UA in the presence (green squares) and absence (blue squares) of 1.0×10^{-4} M AA. Accumulation at open circuit potential for 5.0 min and medium exchange to 0.050 M phosphate buffer solution pH 7.40. Inset: Linear scan voltammograms obtained at GCE/MWCNT-Polyarg in the absence of AA for UA (a) 5.0×10^{-7} M, (b) $8{,}0\times10^{-7}$ M, (c) 1.0×10^{-6} M. (d) 1.25×10^{-6} M, (e) 1.5×10^{-6} M, and (f) 2.0×10^{-6} M. Other conditions as in Figure 2.

petitive since it allows to obtain detection limits lower than most of the sensors presented in the Table.

To study the practical application of the proposed sensor, the MWCNT-Polyarg modified GCE was challenged with human urine samples just diluted with 0.050 M phosphate buffer solution (500 times). The UA concentration obtained after 7 determinations was (15 ± 1) mg dL^{-1}, which is in good agreement (98 %) with the value obtained using the Uricostat Wiener spectrophotometric method (15.4 ± 0.2) mg dL^{-1}.

4 Conclusions

In this work we reported the successful non-covalent functionalization of MWCNTs with Polyarg and the application of GCE modified with MWCNT-Polyarg dispersion for the highly sensitive and selective quantification of UA in the presence of a large excess of AA and in untreated urine samples. GCE/MWCNT-Polyarg is a very versatile and promising (bio)analytical platform that can be used for diverse applications, either by taking advantage of the nanostructures and the charge of the resulting dispersion to quantify negatively charged (bio)analytes or as starting point in the development of more sophisticated biosensors by immobilization of the biorecognition element at the platform.

Electrodes

GCE/HNP-PtTi	GCE modified with hierarchical nanopopous PtTi alloy

GCE/MWCNT/ CTAB-GO	hexadecyl trimethyl ammonium bromide functionalized graphene oxide decorated glassy carbon electrode
GCE/C_{60}/Pt NSs	glassy carbon electrode modified with fullerene/ platinum nanosheets
GCE/MGF/ MWCNT	multiwalled carbon nanotubes and mesocellular graphene foam decorated glassy carbon electrode
GCE/RGO/Au	gold nanoplates and reduced graphene oxide decorated glassy carbon electrode
GCE/RGO	reduced graphene oxide modified glassy carbon electrode
TMB-Cu^{2+}-uricase	colorimetric sensing platform, Cu^{2+}-catalyzed 3,3,5,5-tetramethylbenzidine–H_2O_2 system
GCE/CdTe QDs-Gr	quantum dots CdTe and graphene nanocomposite decorated glassy carbon electrode
GCE/PLL/ERGO	electrodeposited reduced graphene oxide/polymerized L-lysine/modified glassy carbon electrode
AgNP/Zeo-Y/GCE	silver nanoparticles/zeolite Y/modified glassy carbon electrode
GCE/rGo/PAM	polyacrylamide/reduced graphene oxide nanocomposite onto glassy carbon electrode
GCE/Nafion/ MWCNT/CD/HPU	nafion-MWCNT nanocomposite film/electropolymerized β-cyclodextrin/hydrothane polyurethane/modified glassy carbon electrode
Au-IDA/Gr-FMN	gold interdigitated microelectrodes/ flavin mononucleotide – graphene flakes
Au-IDA/Pt-Gr-FMN	gold interdigitated microelectrodes/ flavin mononucleotide – graphene flakes and platinum nanoparticles
GCE/CoPc/ MWCNT	cobalt phthalocyanine/multiwalled carbon nanotube composite
GCE/MoS_2	glassy carbon electrode/molybdenum disulfide nanosheets
GCE/Co-CeO_2	glassy carbon electrode/cobalt doped CeO_2 nanoparticules
GCE-GNs-Q-AgNPs	quercetin /silver nanoparticles/graphene nanosheets/glassy carbon electrode
GCE/Mn-SnO_2/	glassy carbon electrode/Mn doped SnO_2 nanoparticles
GF@$NiCo_2O_4$:GF	graphene/$NiCo_2O_4$ nanowires
GCE/P(GBHA)	glassy carbon electrode/poly(glioxal-bis(2-hydroxyanil)
GCE/C/Ni	carbon-supported Ni nanoparticles/ glassy carbon electrode

Acknowledgements

The authors thank CONICET, ANPCyT, SECyT-UNC, Ministerio de Ciencia y Tecnología de Córdoba for the financial support. A.G. thanks CONICET for the post-doctoral fellowship.

References

[1] J. N. Tiwari, V. Vij, K. C. Kemp, K. S. Kim, *ACS Nano* **2016**, *10*, 46–80.
[2] E. N. Primo, F. Gutierrez, M. D. Rubianes, N. F. Ferreyra, M. C. Rodríguez, M. L. Pedano, A. Gasnier, A. Gutierrez, M. Eguílaz, P. Dalmasso, G. Luque, S. Bollo, C. Parrado, G. A. Rivas in *Electrochemistry of Carbon Electrodes: Electrochemistry in one dimension: applications of carbon nanotubes*, (Eds. R. C. Alkire, P. N. Bartlett, J. Lipkowski, Wiley-VCH Verlag GmbH & Co.KGaA, Weinheim, **2015**, pp. 83–119.
[3] V. Georgakilas, J. A. Perman, J. Tucek, R. Zboril, *Chem. Rev.* **2015**, *115*, 4744–4822.
[4] Z. Li, Z. Liu, H. Sun, C. Gao, *Chem. Rev.* **2015**, *115*, 7046–7177.
[5] N. Yang, G. M. Swain, X. Jiang, *Electroanalysis* **2016**, *28*, 27–34.
[6] T. Feng, Y. Wang, X. Qiao, *Electroanalysis* **2017**, *29*, 662–675.
[7] L. Wang, M. Pumera, *Appl. Mater. Today* **2016**, *5*, 134–141.
[8] P. Yáñez-Sedeño, A. González-Cortés, L. Agüí, J. M. Pingarrón, *Electroanalysis* **2016**, *28*, 1679–1691.
[9] C. Gao, Z. Guo, J.-H. Liu, X.-J. Huang, *Nanoscale* **2012**, *4*, 1948–1963.
[10] S. W. Kim, T. Kim, Y. S. Kim, H. S. Choi, H. J. Lim, S. J. Yang, C. R. Park, *Carbon* **2012**, *50*, 3–33.
[11] E. N. Primo, F. A. Gutierrez, G. L. Luque, P. R. Dalmasso, A. Gasnier, Y. Jalit, M. Moreno, M. V. Bracamonte, M. E. Rubio, M. L. Pedano, M. C. Rodríguez, N. F. Ferreyra, M. D. Rubianes, S. Bollo, G. A. Rivas, *Anal. Chim. Acta* **2013**, *805*, 19–35.
[12] D. Baskaran, J. W. Mays, M. S. Bratcher, *Chem. Mater.* **2005**, *17*, 3389–3397.
[13] M. D. Rubianes, G. A. Rivas. *Electrochem. Commun.* **2007**, *9*, 480–484.
[14] M. Eguílaz, N. F. Ferreyra, G. A. Rivas. *Electroanalysis* **2014**, *26*, 2434–2444.
[15] Y. Jalit, M. C. Rodríguez, M. D. Rubianes, S. Bollo, G. A. Rivas. *Electroanalysis* **2008**, *20*, 1623–1631.
[16] Y. Jalit, M. Moreno, F. A. Gutierrez, A. Sanchez Arribas, M. Chicharro, E. Bermejo, A. Zapardiel, C. Parrado, G. A. Rivas, M. C. Rodríguez. *Electroanalysis* **2013**, *25*, 1116–1121.
[17] P. Dalmasso, M. L. Pedano, G. A. Rivas. *Anal. Chim. Acta* **2012**, *710*, 58–64.
[18] P. Dalmasso, M. L. Pedano, G. A. Rivas. *Biosens. Bioelectron.* **2013**, *39*, 76–81.
[19] F. Gutiérrez, M. D. Rubianes, G. A. Rivas, *Sens. Actuators* **2012**, *161*, 191–197.
[20] E. N. Primo, P. Cañete Rosales, S. Bollo, M. D. Rubianes, G. A. Rivas. *Col. Surf. B: Biointer.* **2013**, *108*, 329–336.
[21] E. Primo, F. Gutierrez, M. D. Rubianes, G. A. Rivas. *Electrochim. Acta*, **2015**, *182*, 391–397.
[22] M. Eguílaz, C. J. Venegas, A. Gutiérrez, G. A. Rivas, S. Bollo, *Microchem. J.* **2016**, *128*, 161–165.
[23] M. Eguílaz, A. Gutiérrez, F. Gutierrez, J. M. González-Domínguez, A. Ansón-Casaos, J. Hernández-Ferrer, N. F.

Ferreyra, M. T. Martínez, G. Rivas, *Anal. Chim. Acta* **2016**, *909*, 51–59.
[24] J. S. N. Dutt, M. F. Cardosi, C. Livingstone, J. Davis. *Electroanalysis* **2005**, *17*, 1233–1243.
[25] J. Fang, M. H. Alderman, *J. Am. Med. Assoc.* **2000**, *283*, 2404–2410.
[26] B. Huang, J. Liu, L. Lai, F. Yu, X. Ying, B.-C. Ye, Y. Li, *J. Electroanal. Chem.* **2017**, *801*, 129–134.
[27] L. Fu, A. Wang, G. Lai, W. Su, F. Malherbe, J. Yu, C.-T. Lin, A. Yu, *Talanta* **2018**, *801*, 248–253.
[28] S. Y. Chu, *J. Med. Technol.* **1978**, *40/5*, 154.
[29] R. L. McCreery, *Chem. Rev.* **2008**, *108*, 2646–2687.
[30] D. Zhao, G. Yu, K. Tian, C. Xu, *Biosens. Bioelec.* **2016**, *82*, 119–126.
[31] Y. J. Yang, W. Li, *Biosens. Bioelectron.* **2014**, *56*, 300–306.
[32] X. Zhang, L.-X. Ma, Y.-C. Zhang, *Electrochim. Acta* **2015**, *177*, 118–127.
[33] H. Li, Y. Wang, D. Ye, J. Luo, B. Su, S. Zhang, J. Kong, *Talanta* **2014**, *127*, 255–261.
[34] C. Wang, J. Du, H. Wang, C. Zou, F. Jiang, P. Yang, Y. Du, *Sens. Actuators* **2014**, *204*, 302–309.
[35] H. Wang, F. Ren, C. Wang, B. Yang, D. Bin, K. Zhang, Y. Du, *RCS Adv.* **2014**, *4*, 26895.
[36] H.-W. Yu, J.-H. Jiang, Z. Zhang, G.-C. Wan, Z.-Y. Liu, D. Chang, H.-Z. Pan, *Anal. Biochem.* **2017**, *519*, 92–99.
[37] D. Zhang, L. Li, W. Ma, X. Chen, Y. Zhang, *Mat. Sci. Eng. C* **2017**, *70*, 241–249.
[38] S. Meenakshi, S. Devi, K. Pandian, R. Devendiran, M. Selvaraj, *Mat. Sci. Eng. C* **2016**, *69*, 85–94.
[39] Y. J. Yang, *Electrochim. Acta* **2014**, *146*, 23–29.
[40] M. B. Wayu, L. T. DiPasquale, M. A. Schwarzmann, S. D. Gillespie, M. C. Leopold, *J. Electroanal. Chem.* **2016**, *783*, 192–200.
[41] A. Abellán-Llobregat, M. Ayán-Varela, L. Vidal, J. I. Paredes, S. Villar-Rodil, A. Canals, E. Morallón, *J. Electroanal. Chem.* **2016**, *783*, 41–48.
[42] J. F. Giarola, A. C. Pereira, *Electroanalysis* **2016**, *28*, 1348–1355.
[43] A. Yin, X. Wei, Y. Cao, H. Li, *Appl. Surf. Sci.* **2016**, *385*, 63–71.
[44] N. Lavanya, C. Sekar, R. Murugan, G. Ravi, *Mat. Sci. Eng. C* **2016**, *65*, 278–286.
[45] H. R. Zare, F. J. -Dehaghani, Z. Shekari, A. Benvidi, *Appl. Surf. Sci.* **2016**, *375*, 169–178.
[46] N. Lavanya, E. Fazio, F. Neri, A. Bonita, S. G. Leonardi, G. Neri, C. Sekar, *J. Electroanal. Chem.* **2016**, *770*, 23–32.
[47] W. Cai, J. Lai, T. Lai, H. Xie, J. Ye, *Sens. Actuators* **2016**, *224*, 225–232.
[48] E. Ergün, Ş. Kart, D. K. Zeybek, B. Zeybek, *Sens. Actuators* **2016**, *224*, 55–64.
[49] W. He, Y. Ding, W. Zhang, L. Ji, X. Zhang, F. Yang, *J. Electroanal. Chem.* **2016**, *775*, 205–211.

Received: January 15, 2018
Accepted: March 6, 2018
Published online on ■■, ■■■

FULL PAPER

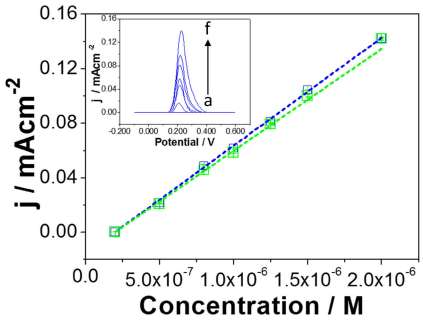

*A. Gutiérrez, F. Gutierrez, M. Egúlaz, C. Parrado, G. A. Rivas**